

Recent Developments on Silicon Photomultipliers produced at FBK-irst

C. Piemonte, M. Boscardin, G.-F. Dalla Betta, *Senior Member IEEE*, M. Melchiorri, N. Zorzi, R. Battiston, A. Del Guerra, *Senior Member IEEE*, G. Llosa

Abstract—In this contribution, new developments on the silicon photomultipliers (SiPM) fabricated at FBK-irst (Trento, Italy) are reported. With respect to the first series of devices produced in 2005/2006, there have been major improvements on both the layout and the technology. Concerning the first aspect we fabricated SiPMs with increased fill factor and with different geometries (square/circular devices, arrays and matrices of SiPMs) to meet the requirements of different applications. Concerning the technology, we identified a process technique able to reduce significantly the dark count rate. In this paper we will describe the main electro-optical characteristics of these devices.

I. INTRODUCTION

In the past few years a growing attention has been devoted to a solid state version of the photo-multiplier tube (PMT), generally referred to as the silicon photomultiplier (SiPM). Compared to PMTs it presents important advantages, such as: compactness, ruggedness, low operational voltage, insensitivity to magnetic fields and low cost. On the other hand, a lot of development is still needed to reach both the noise level (dark count rate) of a PMT as well as to increase the area covered by the device.

FBK-irst (former ITC-irst, Trento) have been developing this device in its own fabrication laboratory since 2005 [1,2]. This is done in collaboration with INFN, which is mainly interested in the application of the sensor in high-energy physics, nuclear medicine and astro physics.

At the 2006 IEEE Nuclear Science Symposium we presented the electro-optical characteristics of the first prototypes of Silicon Photomultipliers produced at FBK-irst, (see [3]). The devices under test had an area of $1 \times 1 \text{mm}^2$ with 625 micro-cells. The fill factor was not optimized yet and its maximum value was about 30%. The electrical characteristics of such devices can be summarized as follows:

- Breakdown voltage of about 30V;

- Dark count rate (DC) increasing linearly with the excess bias voltage (up to 4V); at 3/4V over-voltage, suggested operational point at room temperature, the dark count is about 2.5MHz;
- Optical cross-talk rate less than 5% of the dark count rate at 5V over-voltage;

The optical performance was tested as well. In particular, the photo-detection efficiency (PDE) under constant, low-level (few 10^7 photons/ mm^2/s) illumination was evaluated. The PDE of a SiPM with about 20% fill factor features a peak of about 13-14% in the wavelength range from 460 to 620nm at 4V overvoltage. On the short wavelength side the PDE decreases linearly halving at about 390nm.

In this contribution, we will present the new developments related to the FBK-irst SiPMs. In fact, since 2006 there have been major improvements:

- on the layout side with an optimization of the fill factor;
- on the technological side with a significant reduction of the dark count rate.

II. FEATURES OF THE NEW DEVICES

During 2007 we manufactured a new set of devices featuring an increased fill factor to improve the photo-detection efficiency. In particular, for micro-cell sizes of 40×40 , 50×50 and $100 \times 100 \mu\text{m}^2$ the new values are 40, 50 and 76% respectively. Using these micro-cells we produced SiPMs with different application-oriented geometries:

- square with an area of 1, 4, 9, and 16mm^2 ;
- circular with a diameter of 1.2 and 2.8mm;
- 8, 16, 32-element arrays of $1 \times 0.25 \text{mm}^2$ SiPMs;
- 4×4 -element matrices of $1 \times 1 \text{mm}^2$ SiPMs.

We will focus our attention on the performance of the smallest and largest square devices having an area respectively of 1 and 16mm^2 and a micro-cell size of $50 \times 50 \mu\text{m}^2$. The aim is to demonstrate that the largest SiPM ever produced in our laboratory is fully functional and with characteristics compatible with the smaller one.

The read-out set-up consists in a wide-band voltage amplifier having a 50ohm input resistance connected in series to the SiPM. The amplifier output is then connected to a digital oscilloscope to analyze the signal shape and perform the data analysis. The device is placed in a climatic chamber to control the ambient temperature.

Manuscript received November 21, 2007. This work was supported in part by the INFN-DASiPM project within the MEMS agreement between the Provincia Autonoma di Trento (PAT) and the National Institute for Nuclear Research (INFN).

C. Piemonte, M. Boscardin, M. Melchiorri, N. Zorzi are with FBK, via Sommarive 18, 38050 - Trento, Italy (telephone: +39-0461-314-428, e-mail: piemonte@itc.it).

G-F Dalla Betta is with University of Trento, Department of Information Engineering and Computer Science, and INFN Sezione di Padova (Gruppo collegato di Trento), Via Sommarive 14, I-38050 Povo di Trento, Italy.

R. Battiston is with Università di Perugia, and INFN sezione di Perugia, I-06123 Perugia, Italy.

A. Del Guerra and G. Llosa are with Dipartimento di Fisica 'E. Fermi' and INFN sezione di Pisa, Largo B. Pontecorvo, 3. I-56127, Pisa, Italy.

A. $1 \times 1 \text{mm}^2$ SiPM

This device is composed by 400 $50 \times 50 \mu\text{m}^2$ micro-cells. The normalized scope signal is shown in Fig. 1 in logarithmic scale.

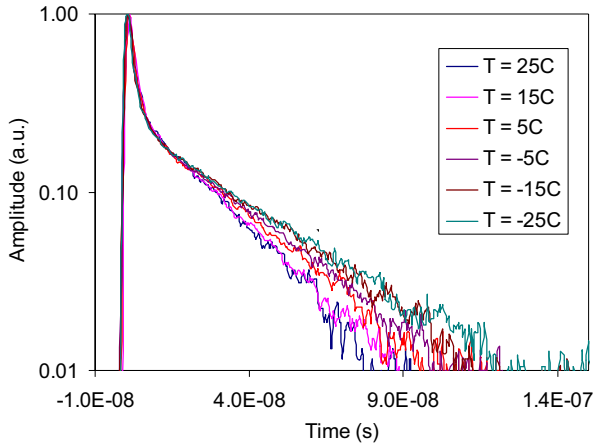


Fig1. Signal shape of the 1mm^2 SiPM at different temperatures.

The trailing edge has two components. The fast transient is a filtered replica of the avalanche current developing at the junction which is visible at the output thanks to a parasitic capacitance in parallel with the quenching resistance. This parasitic element is formed by the coupling of the diode both with the polysilicon resistor and the metal layer. The slow exponential component (straight line in log scale) is determined by the recharge of the junction capacitance through the quenching resistor. It is interesting to note that the recharge time depends on the temperature. This is caused by the temperature dependence of the resistance value, which, due to the polysilicon conduction mechanism, increases with decreasing temperature.

Counting the number of pulses with a threshold level set at half of the signal amplitude it is possible to estimate the dark count (primary dark count + afterpulses with amplitude higher than threshold).

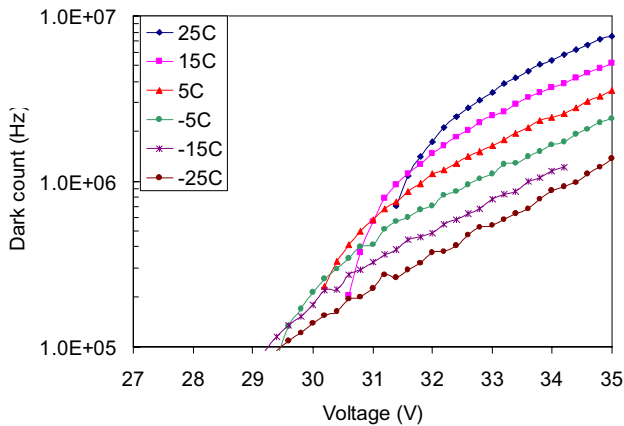


Fig2. Dark count rate as a function of the applied voltage at different temperatures: -25, -15, -5, 5, 15, 25C.

Fig.2 shows the DC as a function of the applied voltage at 6 different temperatures. It is evident that: (i) the breakdown voltage increases with temperature and (ii) the dark count rate decreases with temperature. A clearer picture of the breakdown voltage temperature dependence can be obtained from the gain versus voltage plot shown in Fig. 3.

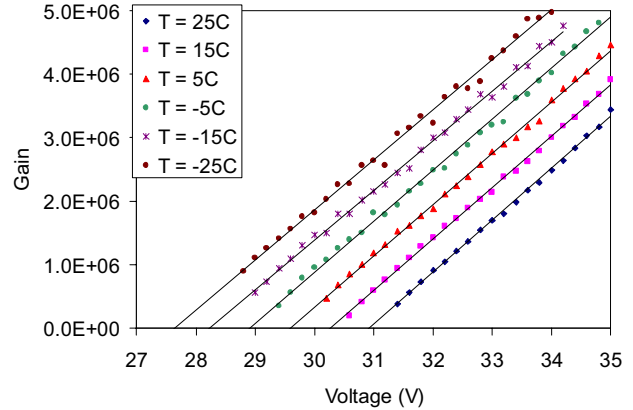


Fig3. Gain vs bias voltage at different temperatures.

The breakdown voltage in this temperature range changes linearly with the temperature with a slope of about 65mV/C . Thus, given a certain bias voltage the gain varies with temperature following a linear coefficient of $50 \times 10^3 \text{ 1/C}$.

B. $4 \times 4 \text{mm}^2$ SiPM

This device is composed by 6400 $50 \times 50 \mu\text{m}^2$ micro-cells.

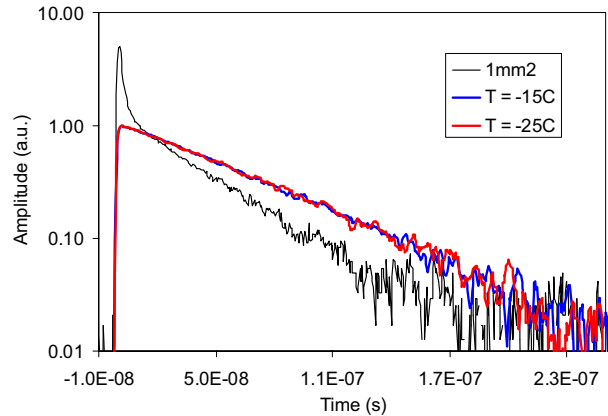


Fig 4. Signal shape of the 16mm^2 SiPM at -15 and -25C. For comparison, the signal of the 1mm^2 device is also shown. The pulses are normalized by their area and then renormalized on the amplitude of the 16mm^2 device.

The pulse shape is rather different from the 1mm^2 device as visible in Fig 4. The fast transient is no longer present and the diode recharge is slower and not temperature dependent. This is caused by the high metal-to-substrate parasitic capacitance (some hundreds of picoFarad) that in parallel with the 50ohm read-out resistor forms a low-pass filter. The filter reshapes the pulse making it slower.

Fig. 5a) and b) show the gain and dark count rate versus voltage characteristics respectively. The measurements are performed only at -15 and -25C in order to have a dark count

level low enough to allow an easy measurement of the two parameters. The gain plot shows, as expected, the same behavior as the smaller device. The dark count scales exactly with the area being 16 times higher than the value found in the 1mm^2 device.

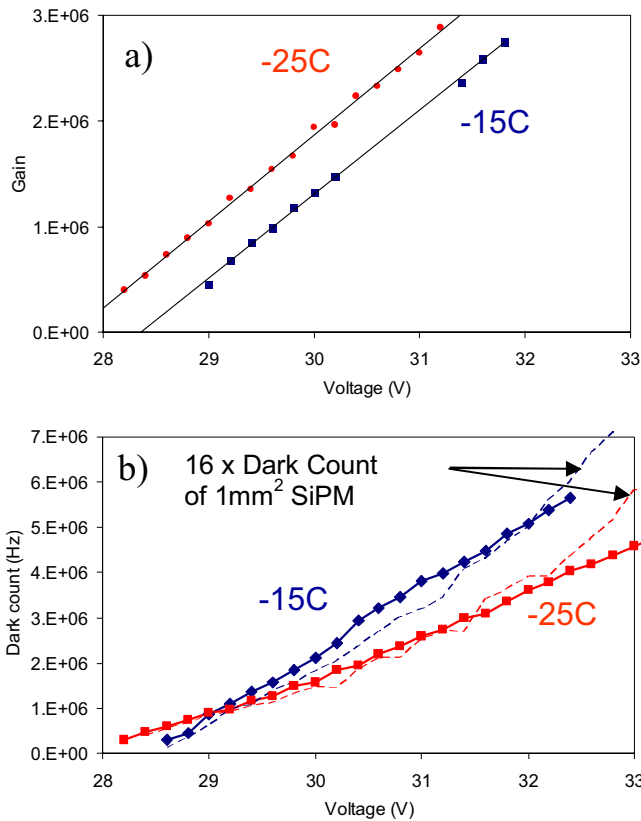


Fig 5. Gain vs voltage and Dark count vs voltage characteristics of the $4\times 4\text{mm}^2$ device at -15 and -25C.

One more point to be verified is the response cell uniformity over such a large number of cells. This can be done measuring the charge of the signal when the device is illuminated with short low-level light pulses. In our set-up we used a blue LED driven by a pulse generator to obtain light pulses with a duration of about 20ns. We integrated the signal over a time of 200ns and collected the histogram of the measured areas. The resulting plots at three different bias voltages are shown in Fig. 6. The measurement is performed at a temperature of -25C and the illumination condition is the same for the three plots. The first peak on the left of each plot is the pedestal and its width is a measure of the electronic noise. The pedestal width increases with the bias voltage because the shot noise due to the current flowing through the device increases. The other peaks correspond to a certain number of activated cells, as evidenced by the labels aside each of them. The width of the peaks is largely dominated by the electronic noise meaning that the uniformity of the cells is excellent.

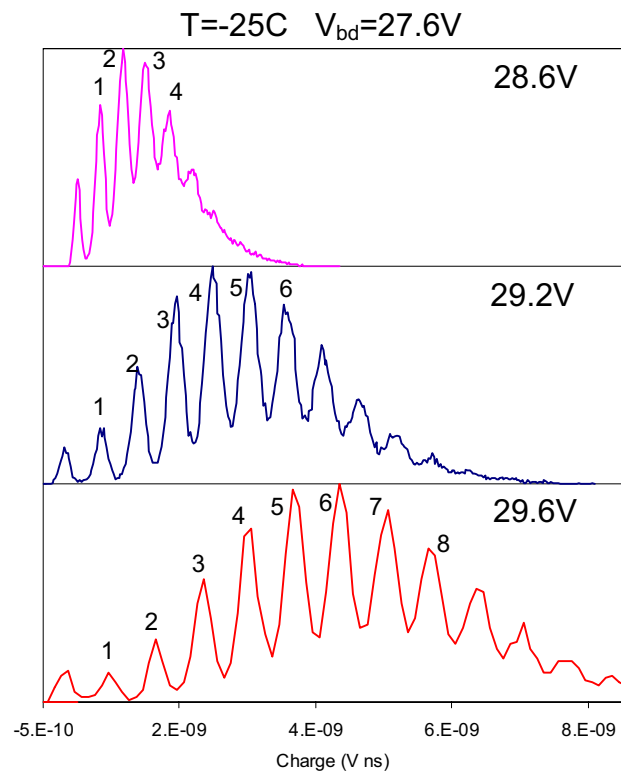


Fig 6. Charge histogram of the SiPM response to low-level short light pulses. The 3 plots correspond to different bias voltages.

C. PDE

The photo-detection efficiency of the two above-described devices is the same because the micro-cell characteristics are the same. The PDE was evaluated on $1\times 1\text{mm}^2$ samples using a photon counting technique [3,4]. This means that we illuminated the SiPM with a constant, very low rate and calibrated flux of photons and we counted the number of signals at the amplifier output. The number of detected pulses (corrected by the dark rate) divided by the number of incident photons gives the PDE.

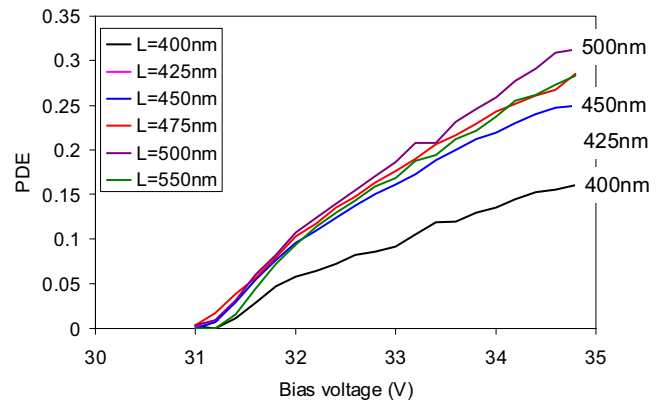


Fig 7. Photo-detection efficiency versus bias voltage at wavelengths ranging from 400 to 550nm of devices having a micro-cell size of $50\times 50\mu\text{m}^2$.

We put particular attention in trying to eliminate the contribution of the after-pulses which increases artificially the PDE at high over-voltages. Fig. 7 shows the PDE as a function of the bias voltage at different wavelengths. As already reported (see [3,4]) the maximum efficiency is reached between 450 and 600nm. With respect to the first devices produced in 2005/06 the maximum value is greatly improved approaching about 30% at 4V over-voltage. This improvement is directly linked to the increased fill factor.

III. NEW TECHNOLOGY

As mentioned in the first section we are currently developing a fabrication process to reduce the dark count rate. In particular, we are studying the most appropriate gettering technique. The dark count rate of devices coming from the first process tests is shown in Fig. 8. The measurement is performed at different temperatures ranging from -5°C to 25°C .

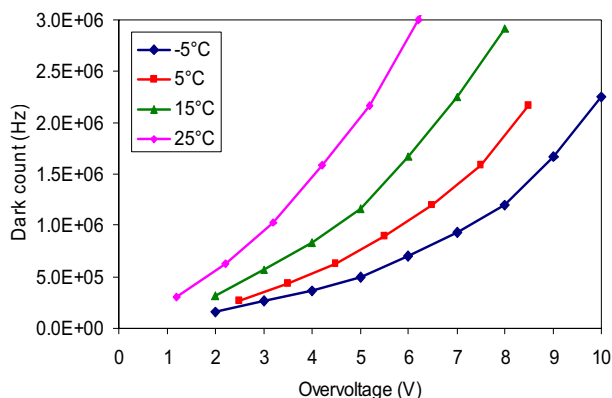


Fig. 8. Dark count rate versus over-voltage at different temperatures.

The improvement with respect to the previous prototypes is significant: the dark count rate is reduced by more than a factor of two; at 3V over-voltage, 25°C , it is at the level of 1MHz. It is important to evidence that we were able to bias the devices at 10V over-voltage at -5°C having a dark count rate of 2MHz. It is important to stress that we measured the dark count on several devices and it was found to be very uniform.

We performed also stability measurements. The measurement consists in keeping the SiPM biased above the breakdown voltage in dark condition for several hours and monitoring the current. Since the current is determined both by the gain and the dark count rate, such test is a fast way to check the stability of the device. We performed this test on several devices and verified that in 1 week of continuous operation the current level did not show any variation.

The uniformity of the response of the micro-cells within a device is extremely good, as demonstrated in Fig. 9, which shows the histogram of the number of photons detected during short light pulses with three different intensities.

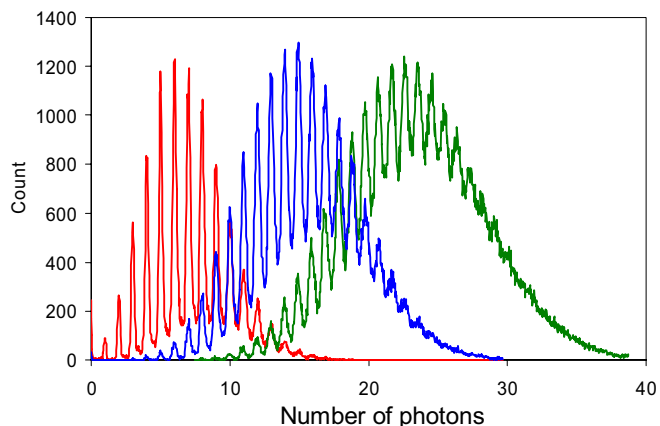


Fig. 9. SiPM response under illumination with short blue light pulses. The three curves correspond to three different light intensities. The device is biased at 4V overvoltage.

Peaks corresponding to more than 20 active microcells are clearly visible.

IV. CONCLUSION

In this paper we reported on the results of the work carried out at FBK on Silicon Photomultipliers in 2007. With respect to the first prototypes we produced devices with improved fill factor as well as application-oriented geometries. We showed that large area devices (up to 16mm^2) work properly having an excellent micro-cell response uniformity. We measured a photo-detection efficiency of about 30% at light wavelengths between 475 and 550nm for a micro-cell size of $50\times 50\mu\text{m}^2$. We are currently developing a process with a lower dark count rate and first results are encouraging. New batches are under production with innovative solutions.

REFERENCES

- [1] C. Piemonte, "A new Silicon Photomultiplier structure for blue light detection" *Nuclear Instruments & Methods*, vol. A568 (2006), pp. 224-232.
- [2] C. Piemonte, R. Battiston, M. Boscardin et al., "Characterization of the First Prototypes of Silicon Photomultiplier Fabricated at ITC-irst" *IEEE Trans. on Nucl. Science*, Vol. 54, N. 1 February 2007, pp. 236-244.
- [3] C. Piemonte, et al., "New results on the characterization of ITC-irst Silicon Photomultipliers", *IEEE Nuclear Science Symposium and Medical Imaging Conference (NSS-MIC'06)*, Conference Record, Paper N42-4, San Diego, California, 29 october-4 november 2006.
- [4] G. Collazuol, et al., "Single photon timing resolution and detection efficiency of the IRST silicon photomultipliers", *Nuclear Instruments & Methods*, vol. A581 (2007), pp. 461-464.